Journal of Physiology (1991), **435**, *pp.* 275–293
With 9 figures
Printed in Great Britain

PATCH CLAMP ANALYSIS OF EXCITATORY SYNAPTIC CURRENTS IN GRANULE CELLS OF RAT HIPPOCAMPUS

BY BERNHARD U. KELLER, ARTHUR KONNERTH* AND YOEL YAARI†

From the Max-Planck-Institut für biophysikalische Chemie, 3400 Göttingen, Germany and †Hebrew University-Hadassah Medical School, Jerusalem 91010, Israel

(*Received 26 February 1990*)

SUMMARY

1. Excitatory postsynaptic potentials (EPSPs) and their underlying currents (EPSCs) were recorded from dentate granule cells in thin hippocampal slices of rats using the tight-seal whole-cell recording technique.

2. At resting membrane potentials (*ca* −60 to −70 mV), the EPSCs clearly consisted of a dominant fast and a smaller slow component. The slow EPSC component markedly increased with depolarization. This resulted in a region of negative slope conductance (between −50 and −30 mV) in the peak current–voltage (*I–V*) relation of the dual-component EPSC in most neurones. The EPSCs reversed entirely at $-1{\cdot}2 \pm 2{\cdot}8$ mV ($n = 15$).

3. Using selective antagonists of *N*-methyl-D-aspartate (NMDA) and non-NMDA excitatory amino acid receptors, two pharmacologically distinct components of the natural EPSCs were isolated. The non-NMDA EPSCs displayed a linear *I–V* relation. Their rise times (0·5–1·9 ms) were independent of membrane voltage but seemed to depend critically on the precise dendritic location of the synapse. Their decay was approximated by a single exponential with a time constant ranging from 3 to 9 ms. The time course of these EPSCs was independent of changes in extracellular Mg^{2+}.

4. The NMDA EPSCs displayed a non-linear *I–V* relation. At resting membrane potentials their peak amplitudes were 20 pA and increased steadily with depolarization to −30 mV. At membrane voltages positive to −30 mV the peak *I–V* relation was linear. The rise times of NMDA EPSCs ranged from 4 to 9 ms and were insensitive to membrane voltage.

5. The NMDA EPSCs decayed biexponentially. Both time constants, τ_f and τ_s, increased with depolarization in an exponential manner, τ_s being more voltage dependent than τ_f. Lowering extracellular Mg^{2+} slightly reduced both rate constants but did not completely abolish their voltage sensitivity.

6. Bath application of NMDA to outside-out patches from granule cells induced single channel currents of 52 pS in nominally Mg^{2+}-free solutions. They displayed a burst-like single-channel activity with clusters of bursts lasting several hundreds of milliseconds. Currents through single NMDA receptor channels reversed around 0 mV.

7. The fractional contributions of NMDA and non-NMDA components to peak

* To whom correspondence should be addressed.

MS 8300

currents and synaptic charge transfer were assessed. At resting membrane potential the NMDA EPSC component accounted for 23% of the peak current and for 64% of the synaptic charge transfer. The contribution of the NMDA EPSC component to the synaptic charge transfer strongly increased with small depolarizations from rest.

INTRODUCTION

Recent studies of mammalian central nervous system (CNS) neurones in culture have shown that the three classical receptors to L-glutamate, namely, the *N*-methyl-D-aspartate (NMDA), kainate and α-amino-3-hydroxy-5-methylisoxazole-4-propionic acid (AMPA) (previously called quisqualate) receptors, are linked to different classes of ion channels. The channels gated by NMDA receptors differ from those gated by non-NMDA (i.e. kainate and AMPA) receptors in several features (for review, see Mayer & Westbrook, 1987). Most notably, NMDA receptor channels are blocked by extracellular Mg^{2+} at negative membrane potentials (Nowak, Bregestovski, Ascher, Herbet & Prochiantz, 1984) causing NMDA-induced currents to be strongly voltage dependent under physiological conditions (Mayer, Westbrook & Guthrie, 1984). They are also much more permeable to calcium than non-NMDA receptor channels (MacDermott, Mayer, Westbrook, Smith & Barker, 1986).

Since L-glutamate or analogue excitatory amino acids (EAAs) are principal neurotransmitters in the mammalian CNS (Watkins & Evans, 1981), it is important to identify and quantify the contribution of NMDA and non-NMDA receptor channels to the synaptic conductance in EAA-operated CNS synapses. A pharmacological separation of the two classes of EAA-receptor channels has become feasible due to the recent development of selective non-NMDA receptor antagonists, namely, the quinoxalinediones (Honoré, Davies, Drejer, Fletcher, Jacobsen, Lodge & Nielsen, 1988). They complement several potent NMDA-receptor antagonists (e.g. ω-phosphonates) that have been known for some time (Watkins & Olverman, 1987). Moreover, a thin-slice preparation that allows tight-seal patch clamp recordings to be made on visualized, synaptically connected mammalian CNS neurones *in situ* was recently introduced (Edwards, Konnerth, Sakmann & Takahashi, 1989).

We have employed these novel tools to characterize the receptor channel types underlying the synaptic conductance at excitatory synapses formed by fibres of the perforant path with dentate granule cells in rat hippocampus (Lømo, 1971). We report here that this synaptic conductance is composed of two separable components, attributable to NMDA and non-NMDA receptor channels. The two components differ dramatically in voltage dependence, time course, charge transfer capacity and single-channel properties, supporting the notion that they may subserve different synaptic functions. Some of the results of this study have been presented elsewhere in a preliminary form (Keller, Yaari & Konnerth, 1990).

METHODS

Slice preparation

The procedures of preparing and maintaining thin slices from mammalian CNS and of cleaning cells in the slices for patch clamp recordings have been described in detail elsewhere (Edwards *et al.* 1989). Briefly, brains of 10- to 21-day-old rats were removed after decapitation and blocks of cerebral tissue were cut into thin slices (120–150 μm) with a vibrating slicer (FTB Vibracut,

Germany). From each cerebral slice the portion belonging to the hippocampus was dissected out and transferred to a storage chamber containing oxygenated (95% O_2, 5% CO_2) normal saline at 35 °C. Hippocampal slices were then transferred to a recording chamber placed on the stage of an upright microscope. This chamber was continuously perfused with oxygenated saline solutions

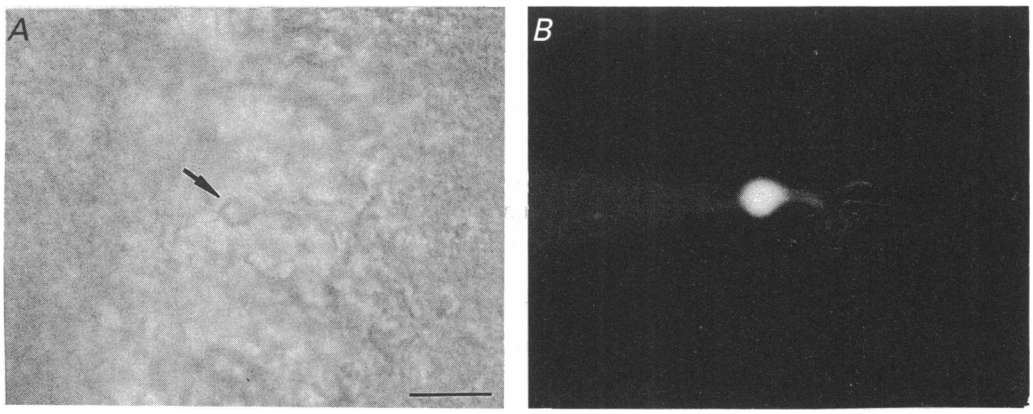

Fig. 1. *A*, photomicrograph of a granule cell of dentate gyrus in a thin rat hippocampal slice viewed under Nomarski optics. The neurone in the centre of the picture was 'cleaned' for patch clamp measurements (×400 magnification; calibration bar = 10 μm). *B*, fluorescence micrograph of the same cell after being patch clamped in the whole-cell configuration with a micropipette containing the dye Lucifer Yellow.

kept at room temperature (21–24 °C). Somata of dentate granule cells were clearly discerned when viewed with Nomarski optics (Zeiss) using a long distance 40 × water immersion objective (Fig. 1). The cells chosen for recording were cleaned from debris by gently blowing on them a stream of saline through the tip (5–10 μm) of a nearby 'cleaning' pipette, followed by sucking the resulting debris into the pipette (Edwards *et al.* 1989). The data presented in this paper summarizes the observations made during stable, long-lasting (≥ 1 h) tight-seal recordings from fifty-four granule cells.

Solutions and drugs

Normal saline contained (in mM): NaCl, 125; KCl, 2·5; $CaCl_2$, 2; $MgCl_2$, 1; NaH_2PO_4, 1·25; $NaHCO_3$, 26; glucose, 20–25 (pH 7·4). $MgCl_2$ was omitted in preparing Mg^{2+}-free saline. However, due to contamination, the latter solution contained 3 μM-ionized Mg^{2+}, as determined fluorimetrically (Konnerth, Keller, Ballanyi & Yaari, 1990*a*). All perfusing solutions contained 10 μM-bicuculline methiodide (Sigma, Germany) to block GABA-mediated inhibitory postsynaptic currents. Additional drugs used were tetrodotoxin (TTX, Sigma), DL-2-aminophosphonovalerate (APV, Sigma), 3-(2-carboxypiperazinyl) propyl-phosphonate (CPP, Tocris Neuramin Ltd) and cyano-nitroquinoxaline-dione (CNQX, Tocris). Drugs were applied to the preparations in the perfusing saline.

The pipette (intracellular) solution contained (in mM): CsCl, 120; tetraethylammonium (TEA), 20; $CaCl_2$, 1; $MgCl_2$, 2; Na-ATP, 4; EGTA, 10; HEPES, 10 (pH 7·3). ATP was included in order to prevent possible run-down of synaptic currents as described by Moody, Salter & MacDonald (1988). Due to strong chelation of Mg^{2+} by ATP ($K_d = 10^4$ at pH 7·2; Martell & Smith, 1974) the intracellular concentration of ionized Mg^{2+} was estimated to be ≤ 1 μM.

Stimulation and recording

Stimulation electrodes made either of thin (25 μm) Teflon-coated platinum wires or fine glass pipettes (tip diameter 4–5 μm) were used for stimulating fibres near the outer border of the dentate granule cell layer. Typically the stimulating electrode was positioned at about 50–200 μm from the recording site. Stimuli of 200 μs duration and 3–8 V stimulation intensity were generated by a stimulation isolation unit and delivered at 0·2 Hz during the sampling period.

Whole-cell tight-seal (seal resistances greater than 10 GΩ) recordings were made in current clamp and voltage clamp modes (Hamill, Marty, Neher, Sakmann & Sigworth, 1981) using patch pipettes with open resistances of 4–5 MΩ and an EPC-7 patch clamp amplifier (List Electronics, Germany). Depending on the measurements to be performed, signals were filtered at 0·5 to 5 kHz with an 8-pole Bessel filter (Frequency Devices, MA, USA) and stored on videotapes by a PCM/VCR recording device (Instrutech, NY, USA).

During patch clamp measurements, the resistance–capacitance (*RC*) network connecting the dendrites to the cell soma will act as a filter for the postsynaptic currents. In order to find an estimate for the filter properties, we applied voltage steps of ±10 mV from a holding potential of −70 mV. In all the cells tested ($n = 6$), the decay of the resulting current response was biphasic and could be described by the sum of two exponential components with time constants of 0·1 ± 0·05 ms (τ_1) and 1·2 ± 0·4 ms (τ_2). Most likely, these components reflect the charge movement necessary to charge the somatic (τ_1) and dendritic (τ_2) membrane capacitance via the *RC* network of the cell (Llano, Marty, Armstrong & Konnerth, 1990). For our purposes, these measurements suggest the following. (i) An approximate membrane capacitance of $C_M = \tau_2/R_s \sim 120$ pF is recharged during the voltage pulse at a series resistance $R_s = 8$–10 MΩ obtained during patch clamp measurements. This capacitance corresponds to a membrane area exceeding the surface area of a sphere with the diameter of the soma ($d \sim 9\ \mu$m) by a factor of 30, suggesting that the proximal dendritic membranes are under voltage clamp control. (ii) For synaptic currents which are evoked at proximal synaptic locations by an appropriate location of the stimulation pipette, the dendritic *RC* filter is negligible, provided that the relevant time constants are large compared to $\tau_2 = 1{\cdot}2$ ms.

Data analysis

Analog signals were digitized off-line at sampling rates between 0·5 and 2 kHz for slow and fast synaptic responses, respectively. Measurements of rise times, peak amplitudes and decay rates were normally performed by averaging five to ten consecutive EPSCs. Curve fitting of single or double exponentials was performed by a family of interactive computer programs (courtesy of B. Sakmann, MPI für Medizinische Forschung, Heidelberg) using a VMEbus computer system or the Instrutech software package using an Atari computer. The synaptic charge transferred during an EPSC was determined by calculating the time integral of individual EPSCs, using parameters obtained from the fitted sum of exponential functions.

RESULTS

Excitatory postsynaptic responses in dentate granule cells

Stimulation of fibres near the border of the dentate granule cell layer consistently produced excitatory postsynaptic responses with a latency of 1–2 ms in whole-cell clamped granule cells. Typical EPSPs and EPSCs recorded from a granule cell in current clamp and voltage clamp modes, respectively, are illustrated in Fig. 2. As seen in both modes of recording, consecutive synaptic responses to a constant stimulus fluctuated in amplitude. This variation may reflect variation in excitability of afferent fibres or in quantal fluctuations of the amount of neurotransmitter released from presynaptic terminals (Andersen, 1987).

Threshold stimulus intensity for obtaining a detectable postsynaptic response was ~ 2 V in most experiments. Higher stimulus intensities (up to 6 V) resulted in larger EPSPs and EPSCs. Exposing preparations to 1 μM-TTX abolished the postsynaptic responses completely, indicating that the stimuli trigger neurotransmitter release by evoking action potentials in afferent fibres, rather than by depolarizing presynaptic terminals directly. Likewise, perfusion with 2 mM-Ni^{2+}, a blocker of calcium channels, markedly suppressed postsynaptic responses (data not shown).

Current–voltage analysis of EPSCs

To investigate the current–voltage (*I–V*) relation of the EPSCs, the granule cells were clamped at voltages ranging from −90 to +50 mV. A representative series of EPSCs obtained at different holding membrane potentials is illustrated in Fig. 3*A*.

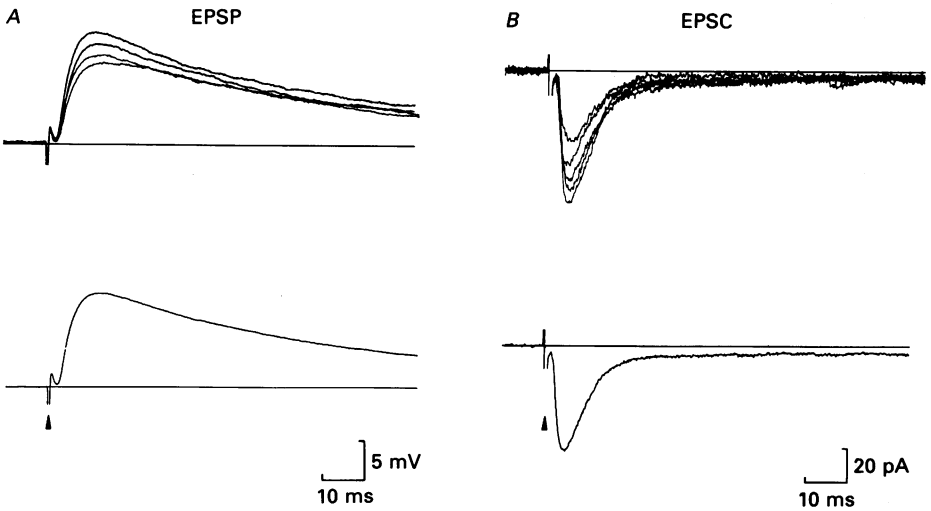

Fig. 2. Excitatory synaptic responses in dentate granule cells. *A*, excitatory postsynaptic potentials were recorded in the whole-cell mode under current clamp conditions during stimulation of the perforant path. Bottom record, computer average of the four EPSPs shown above. *B*, excitatory postsynaptic currents obtained under voltage clamp conditions at a holding voltage of $V_h = -72$ mV. Stimulation parameters 3 V, 200 μs. Bottom record, average of the five EPSPs shown above. Arrow-heads indicate the time of stimulation here and in the following figures.

The *I–V* relation of the peak EPSCs were close to linear over most of the voltage range (slope conductance ~ 4·9 nS), except for a small region of negative slope conductance at membrane potentials between −50 and −30 mV (Fig. 3*B*). Similar N-shaped *I–V* curves were seen in seven cells. However, in four other cells the *I–V* curves of peak EPSCs did not display any conspicuous deviation from linearity (see below, Fig. 9*A*).

The reversal potential of the peak EPSCs was $-1{\cdot}2 \pm 2{\cdot}8$ mV ($n = 15$). This value is close to the reversal potential expected for cation-selective glutamate receptor channels (Hablitz & Langmoen, 1982; Crunelli, Forda & Kelly, 1984; Cull-Candy & Usowicz, 1989*a*, *b*) and is quite similar to previously reported values of reversal potentials of EPSPs in the dentate gyrus ($-5{\cdot}5 \pm 1{\cdot}1$ mV, Crunelli *et al.* 1984).

As illustrated in Fig. 3*A*, the time course of the EPSCs was strongly voltage dependent. At membrane potentials close to, or more negative than, the resting potential (between −90 and −60 mV), the decay time course of the EPSCs in all cells analysed ($n = 54$) was clearly biphasic. The EPSCs first decayed rapidly within a few milliseconds. This was succeeded by a slow decay of the residual EPSCs lasting tens

of milliseconds. As the membrane potential was depolarized, the slowly decaying EPSC component became more and more dominant (Fig. 3*A*). This suggested that EPSCs in granule cells are composed of fast and slow components with different voltage sensitivities, as recently was described in excitatory (presumably

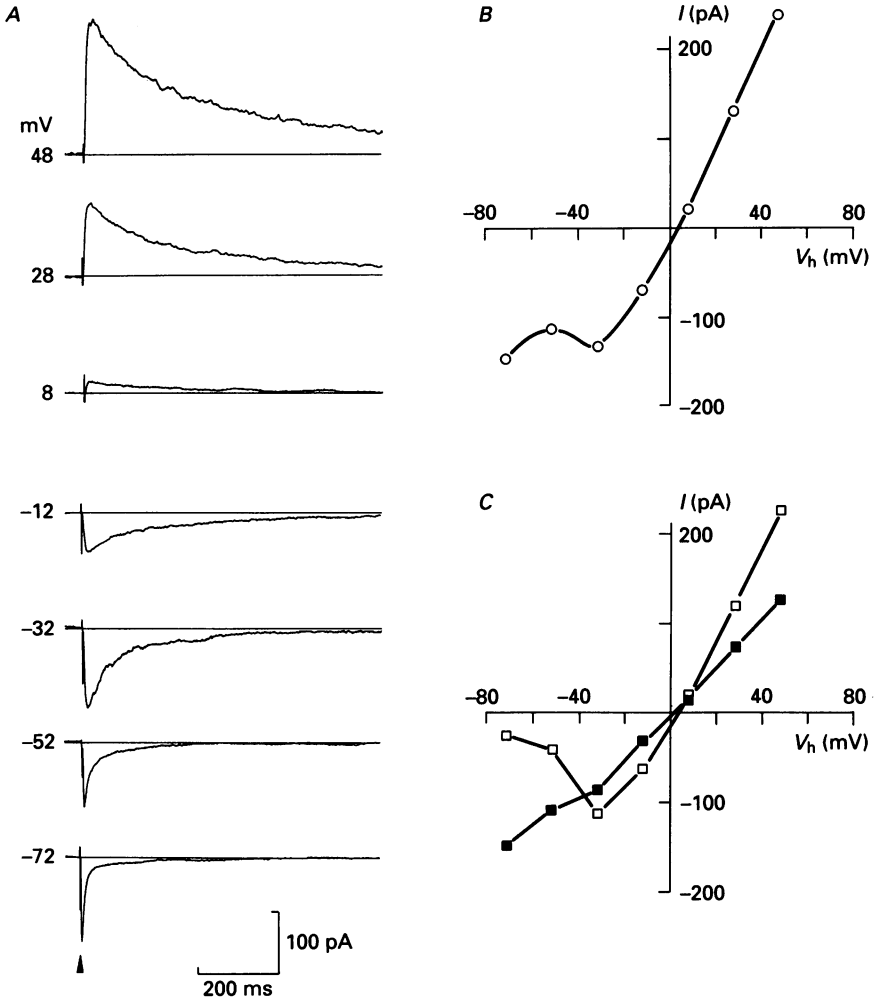

Fig. 3. Voltage dependence of excitatory postsynaptic currents (EPSCs) in dentate granule cells. *A*, EPSCs recorded at different holding potentials (as indicated on the left of each trace) showing (i) the biphasic time course of EPSCs at negative voltages and (ii) the prolongation of EPSC decay at positive voltages. Each trace represents the average of five or six consecutive EPSCs. *B*, peak amplitude of the EPSC as a function of membrane potential. The reversal potential was +2 mV. *C*, EPSC amplitudes as a function of potential for different time windows after stimulation. ■, current–voltage relation of the amplitude taken at the peak of the EPSC at $V_h = -72$ mV (7 ms after stimulation). □, current–voltage relation 21 ms after stimulation. All data shown in this figure were taken from the same experiment.

L-glutamatergic) synapses at spinal and hippocampal neurones in culture (Forsythe & Westbrook, 1988).

In order to delineate fast and slow EPSC components, we measured EPSC amplitudes at different time windows (Fig. 3*C*). The first component, measured at the time of the peak current at resting potential (at 7 ms in the experiment shown in Fig. 3*C*), displayed a linear slope conductance of ~ 0·2 nS over the entire voltage range (■ in Fig. 3*C*). By contrast, the slow EPSC component, given by the current amplitudes at a delay of 21 ms (which corresponds to about 3 times the decay time of the fast component) after stimulation, displayed an *I–V* curve with a prominent region of negative slope conductance at membrane potentials more negative than −30 mV (□ in Fig. 3*C*). At membrane voltages more positive than −30 mV, the *I–V* relation of the slow EPSC component was linear with a slope conductance of 0·4 nS. In all cells thus examined ($n = 11$), including the four cells with linear *I–V* relations of the peak EPSC amplitudes, the EPSCs were similarly separable into fast and slow components. The two components reversed at approximately the same membrane potential (Fig. 3*C*).

Pharmacological isolation of non-NMDA EPSCs

Recent studies of excitatory connections between hippocampal neurones in slices (Andreasen, Lambert & Jensen, 1988, 1989; Blake, Brown & Collingridge, 1988; Herstrin, Nicoll, Perkel & Sah, 1990) and in culture (Forsythe & Westbrook, 1988; Bekkers & Stevens, 1989) have indicated that fast and slow components of presumptive L-glutamate-mediated EPSPs are generated by activation of non-NMDA and NMDA receptors, respectively. We tested the notion that the fast EPSC component is mediated by non-NMDA receptors by blocking NMDA receptors with selective antagonists. As illustrated in Fig. 4*A* and repeated in twelve experiments, application of 50 μM-APV (D-aminophosphonovalerate) suppressed most of the slow component of the EPSCs. Experiments with 10 μM-CPP ($n = 8$) yielded similar results. The remaining EPSC component was entirely abolished by 4 μM-CNQX, thus identifying it as a pure non-NMDA receptor-mediated EPSC.

The *I–V* relation of the peak non-NMDA EPSCs was linear with a slope conductance of 0·1 nS as exemplified in Fig. 4*B*. Its shape was thus similar to the *I–V* relation of the fast component of the compound EPSC (Fig. 3*C*).

Kinetics of non-NMDA EPSCs

The use of the whole-cell patch clamp technique enabled us to study in detail the time course of non-NMDA EPSCs over a large voltage range. Their rise times (10–90 %) were voltage independent and ranged from 0·5 to 1·9 ms. The duration of the rise times was influenced by the location of the synaptic stimulation, suggesting that their variability reflects the filter properties of the dendritic *RC* network rather than the true rise times of the EPSCs (see Methods section). For synaptic currents evoked at proximal synaptic locations (rise time 0·5 ms), the decay time of the fast EPSC could be as fast as 3·2 ms (Fig. 5). However, at more distal synaptic locations indicated by slower rise times (> 1·5 ms), a decay time up to 9·5 ms could be observed.

In those cells which displayed a slow rise time, a second component in the decay of non-NMDA EPSCs was observed as displayed in Fig. 4*A* (trace at +25 mV). This component was prolonged by depolarization and displayed a decay time constant up to 26 ms. Although the decay rates of this component of non-NMDA EPSPs were

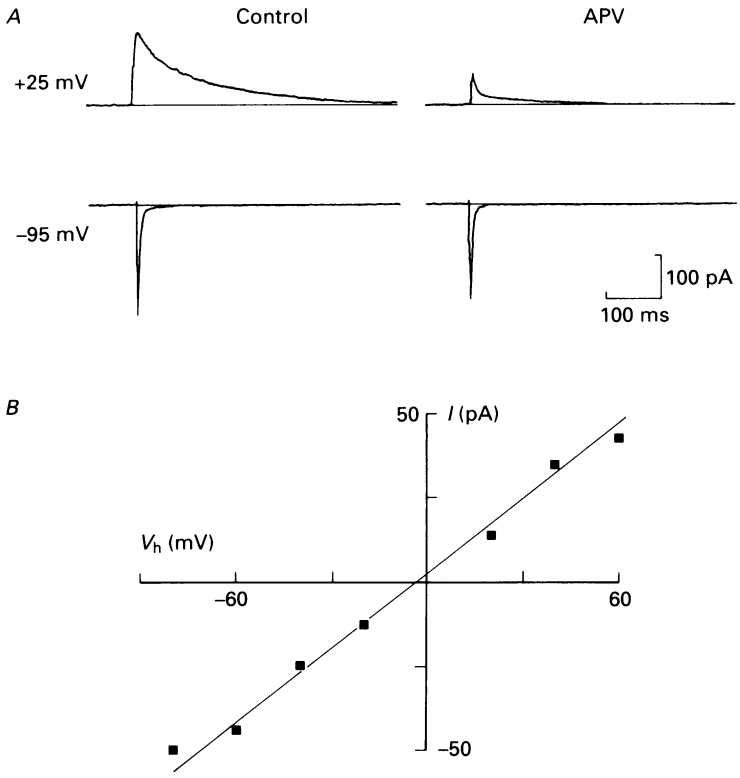

Fig. 4. Pharmacological isolation of the non-NMDA current component. *A*, EPSCs at a negative (−95 mV) and a positive (+25 mV) holding potential before (control) and after application of 50 μM-APV. Current traces correspond to averages of five or six consecutive EPSCs each. *B*, plot of the current–voltage relation of non-NMDA EPSCs recorded in the presence of 10 μM-CPP. The regression line has a linear slope conductance of 0·8 nS (least squares). Extracellular Mg^{2+} concentration was 2 mM in both experiments. The reversal potential was −6 mV.

much faster than the decay rates of NMDA EPSCs, we initially suspected that this component might reflect activation of NMDA receptors insufficiently blocked by CPP or APV. However, doubling the concentrations of extracellular Mg^{2+} (to 2 mM) and of CPP (to 20 μM) did not suppress this component. Furthermore, this component was totally abolished by 5 μM-CNQX, suggesting that it is attributable to activation of non-NMDA receptors. At present, however, we cannot completely rule out that this component might be induced by inadequate voltage-clamp conditions or by a synaptic input with an extensive spatial dispersion. Therefore, we omitted this component from the current analysis.

Pharmacological isolation of NMDA EPSCs

Using the same pharmacological approach described above, we isolated the NMDA receptor-mediated EPSCs (NMDA EPSCs) by blocking the non-NMDA EPSC component with 4 μM-CNQX. As illustrated in Fig. 6, this drug had a profound effect

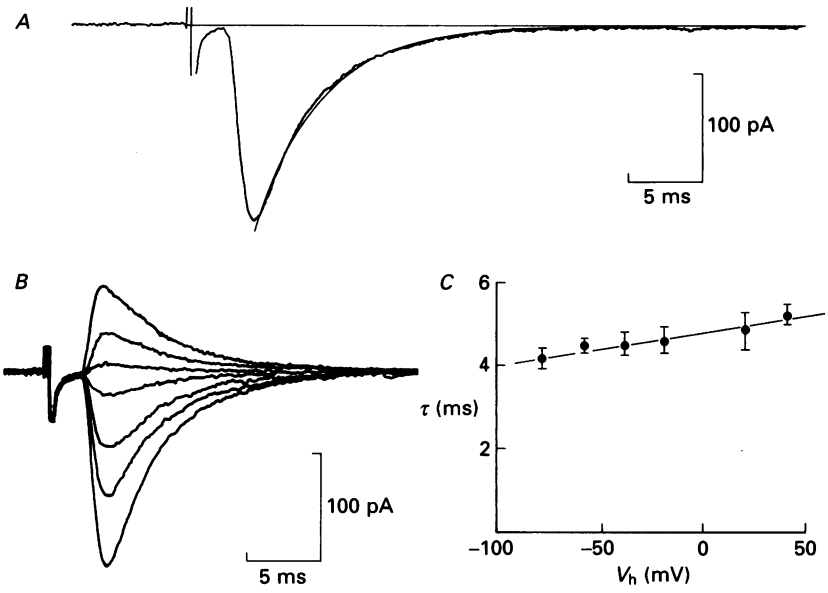

Fig. 5. Time course of non-NMDA receptor-mediated EPSCs. *A*, the decay of the EPSC was well fitted by a single exponential function (continuous line: amplitude = −195 pA, τ = 4·5 ms). Record represents the average of seven EPSCs recorded at V_h = −80 mV in the presence of 10 μM-CPP. *B*, superimposed traces (six to eight averages each) of non-NMDA EPSCs obtained at voltage steps of +20 mV starting from −80 mV (bottom trace). *C*, decay time constant of non-NMDA EPSC plotted as a function of voltage. Continuous line was fitted by eye.

at negative membrane potentials, at which it abolished the fast component of the compound EPSC. At positive membrane potentials the effect of the drug was not apparent (Fig. 6), since at these potentials the dominant component of the EPSC is mediated by NMDA receptor channels. As expected, adding CPP (10 μM) or APV (50 μM) to CNQX-treated preparations blocked the remaining EPSC component entirely.

A representative *I–V* relation of pharmacologically isolated NMDA EPSCs in 1 mM-external Mg^{2+} is illustrated in Fig. 6*B*. An appreciable EPSC component ($\sim$ 20 pA) was consistently seen even at voltages more negative than −60 mV, suggesting that in dentate granule cells a portion of NMDA receptors are synaptically activated at normal resting potentials (Lambert & Jones, 1989). At membrane potentials between −70 and −30 mV, the *I–V* curve of the NMDA EPSCs displayed a negative slope conductance, similar to that seen upon NMDA application to

mammalian CNS neurones in culture (Mayer & Westbrook, 1987). Above −30 mV the *I–V* relation was linear. In all these respects the *I–V* relation of the NMDA EPSCs was identical to the *I–V* curve of the slow component of the compound EPSC (Fig. 3*C*).

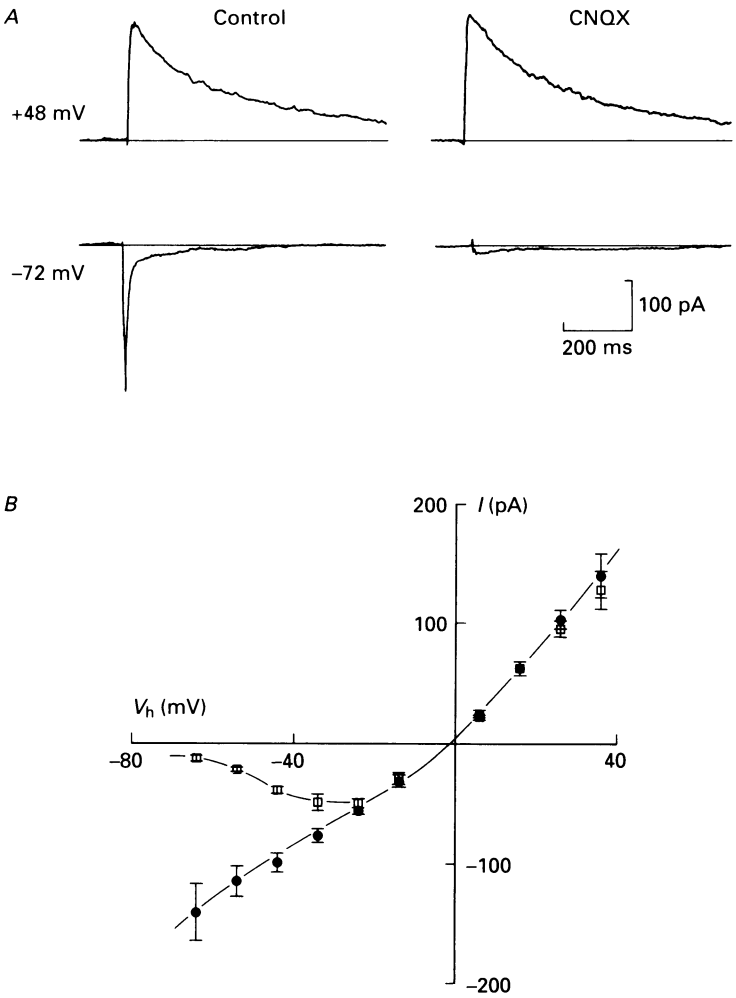

Fig. 6. Pharmacological isolation of NMDA receptor-mediated EPSCs. *A*, EPSCs obtained before and after addition of 5 μM-CNQX to the bath solution in the presence of 1 mM-Mg^{2+} in the external solution. The fast, non-NMDA EPSCs were completely blocked after addition of 5 μM-CNQX as clearly seen at $V_h = -72$ mV, while the dominating NMDA EPSC at $V_h = +48$ mV was much less affected by CNQX. *B*, current–voltage relation for NMDA receptor-mediated EPSCs in the presence of 5 μM-CNQX. □, NMDA-mediated current–voltage curve in the presence of 1 mM-external Mg^{2+}. ●, current–voltage relation of NMDA receptor-mediated EPSC in nominally Mg^{2+}-free solutions.

The negative slope conductance between −70 and −30 mV in the *I–V* relation of NMDA induced currents is due to blockage of NMDA receptor channels by extracellular Mg^{2+} (Mayer *et al.* 1984; Nowak *et al.* 1984). In congruence with this

notion, we found that in nominally Mg^{2+}-free solutions this region in the *I–V* relation of NMDA EPSCs became linear (Fig. 6*B*).

Kinetics of NMDA EPSCs

The rise times (10–90% maximum amplitude) of NMDA EPSCs in 1 mM-Mg^{2+} ranged between 4 and 9 ms (mean = 6·4 ± 1·8 ms; $n = 5$) and did not display a

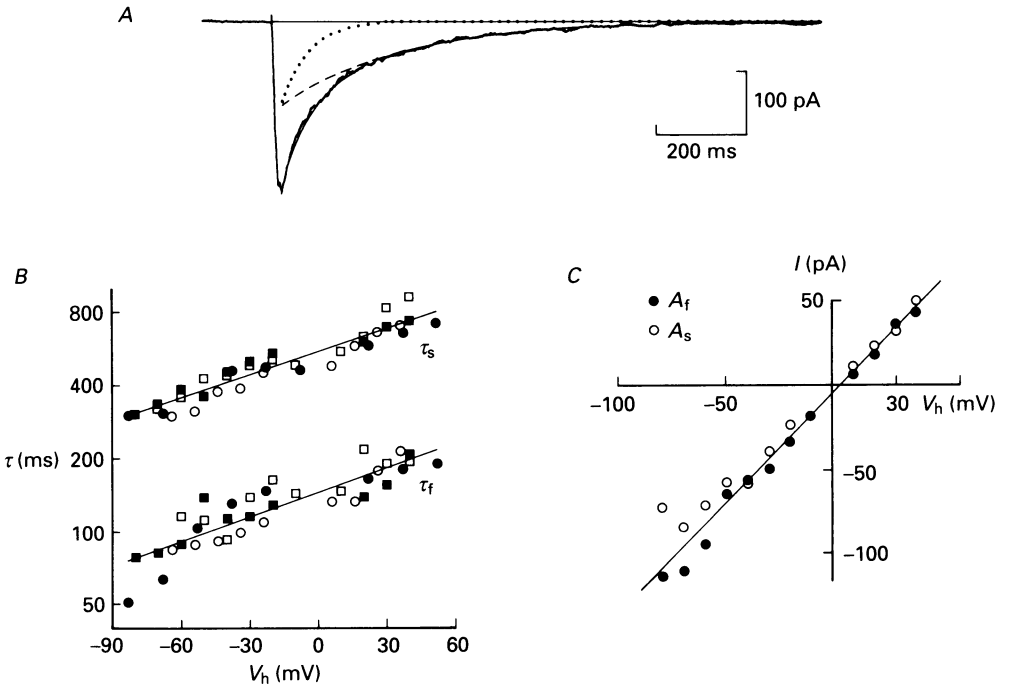

Fig. 7. Voltage dependence of the biexponential decay of NMDA EPSCs. *A*, NMDA EPSC recorded in nominally Mg^{2+}-free solutions at $V_h = -68$ mV was fitted by a biexponential function as described in the Methods section. The continuous line represents the double exponential fit as the sum of the slow component (dashed line) corresponding to $\tau_s =$ 272 ms and $A_s = -135$ pA and the fast component (dotted line) corresponding to $\tau_f =$ 61 ms and $A_f = -129$ pA, respectively. *B*, voltage dependence of both exponential decay time constants τ_f and τ_s. Cumulative data from four experiments are shown. Linear regression yields an e-fold change for voltage steps of 129 ± 15 mV (τ_f) and 134 ± 14 mV (τ_s; $n = 4$) respectively. *C*, current–voltage relation for the amplitudes of the fast (A_f; ●) and slow (A_s; ○) exponential components. Line was drawn by eye.

significant voltage sensitivity. By contrast, the decay time course of these currents was markedly dependent on the holding potential. The decay of NMDA EPSC could be best fitted with a biexponential function having a fast (τ_f) and a slow (τ_s) decay time constant. At −70 mV, the mean values of τ_f and τ_s were 46 ± 13 and 235 ± 38 ms ($n = 4$), respectively. Both τ_f and τ_s increased exponentially with membrane depolarization with an e-fold change for voltage steps of 83 ± 16 mV (τ_f; $n = 4$) and 121 ± 13 mV (τ_s; $n = 4$).

Perfusing the preparations with Mg^{2+}-free solutions markedly increased the decay

time constants (Fig. 7*B*). At −70 mV, τ_f and τ_s were given by 84±18 and 330±34 ms ($n = 4$), respectively. The voltage sensitivity of these time constants was slightly attenuated in this condition with an e-fold increase for voltage steps of 129±15 mV (τ_f; $n = 4$) and 134±14 mV (τ_s; $n = 4$). Both components maintained

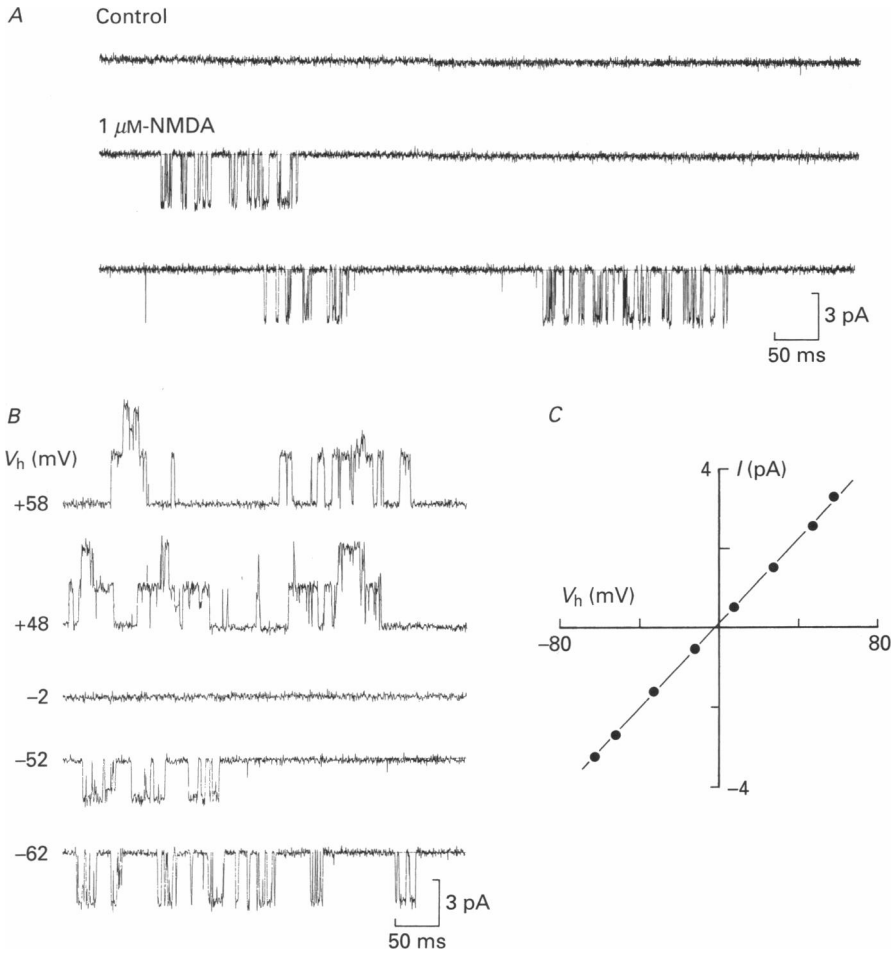

Fig. 8. Unitary activity of NMDA receptor channels in outside-out patches from granule cells in thin-slice preparations. *A*, currents through single NMDA receptor channels recorded in the outside-out patch configuration during bath application of 1 μM-NMDA. Note that opening of NMDA receptor channels occurred in clusters of bursts, each cluster lasting several hundreds of milliseconds. *B*, single-channel currents recorded at different holding potentials indicated at the left of each current trace. *C*, current–voltage relationship for single NMDA receptor channels ($\gamma = 52$ pS; reversal potential = −1·8 mV). Bath solution was normal saline and 1 μM-NMDA. Pipette solution was 120 mM-CsCl, 20 mM-TEA, 1 mM-$CaCl_2$, 2 mM-$MgCl_2$, 4 mM-Na-ATP, 10 mM-EGTA and 10 mM-HEPES (pH 7·3).

their relative contribution with almost equal amplitudes of −95 pA at −70 mV (Fig. 7*C*).

Single-channel recording of NMDA receptor channels

In order to reveal the ionic channel underlying the NMDA EPSC we recorded NMDA induced single-channel currents in the slice preparation. Figure 8 shows

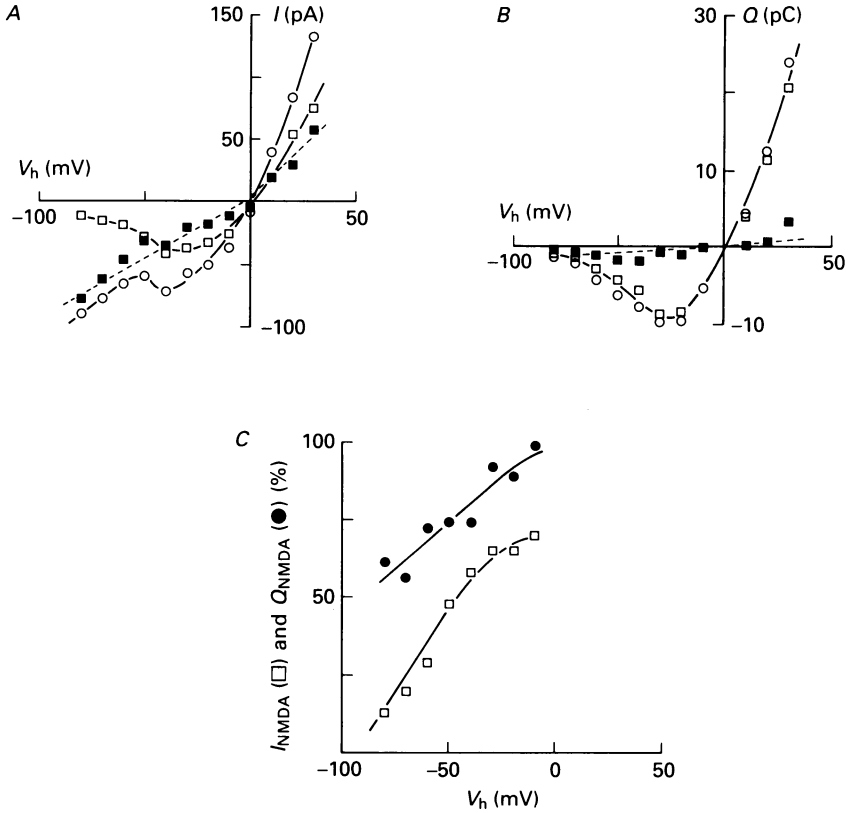

Fig. 9. Contribution of NMDA and non-NMDA receptor activation to the peak current and the total charge carried by the EPSC. *A*, peak currents were determined under control conditions (○) and in the presence of 5 μM-CNQX (NMDA component, □). The non-NMDA component (■) was estimated from the difference in peak current with and without CNQX in the bath. *B*, charge (*Q*) transported by control (○), NMDA (□) and non-NMDA (■)-mediated EPSCs. Charge contributions were determined by exponential fitting of the decay of the EPSCs and determining the area under each curve as the product of amplitude and the corresponding decay time constant. *C*, relative contribution of NMDA component to peak current (I_{NMDA}, □) and charge transport (Q_{NMDA}, ●) for the data shown in *A* and *B*.

NMDA induced single-channel activity obtained in an outside-out patch from granule cells retained in nominally Mg^{2+}-free solutions under conditions similar to those in which EPSCs were recorded. Single-channel activity recorded during bath

application of 1 μM-NMDA displayed a main conductance level around 52 pS (52 ± 2, $n = 5$). Occasionally, subconductance levels were observed, but have not been analysed so far. In all patches analysed ($n = 5$), channel openings appeared in clusters of bursts lasting several hundreds of milliseconds (Fig. 8*A*). The reversal potential of the single-channel currents was close to 0 mV ($n = 5$, Fig. 8).

Contribution of NMDA and non-NMDA receptor-mediated activity to the EPSC

The pharmacological experiments clearly delineated two EPSC components in hippocampal granule cells, namely a non-NMDA EPSC and a NMDA EPSC, that differ in their kinetics and voltage dependences. To assess the contribution of the two components at different membrane potentials, we measured EPSC amplitudes at the peak times of the natural EPSCs before (Fig. 9*A*, ○) and after CNQX application. The amplitudes measured in CNQX represented the NMDA-mediated fraction of peak current (Fig. 9*A*, □). Subtracting these values from the control amplitudes provided the non-NMDA-mediated fraction of peak current (Fig. 9*A*, ■). Using the same approach we estimated the contribution of the two EPSC components to the total synaptic charge transfer (Fig. 9*B*, ○). The synaptic charge transferred through non-NMDA receptor channels (Fig. 9*B*, ■) was calculated by deducing the contribution of the NMDA component (measured in CNQX; Fig. 9*B*, □) from control values. The contribution of the NMDA EPSC to synaptic charge transfer was dominant, particularly for voltages positive to −60 mV.

The fractional contributions of the NMDA component to current and charge transport are plotted in Fig. 9*C*. It is evident that at membrane voltages close to resting potential, only a small fraction of the peak current flows through NMDA receptor channels (□). At resting potential, 23 % of the peak current is mediated by NMDA EPSCs. The contribution of this component to peak EPSCs steadily increases with depolarization and becomes dominant at positive voltages. The fractional contribution of NMDA EPSCs to the transferred charge is shown as filled circles in Fig. 9*C*. Even at resting potential this component accounts for more than 64 % of the charge transfer. The contribution of this component increases steeply with depolarization, accounting for up to 94 % of the charge transferred during an EPSC (Fig. 9*C*).

DISCUSSION

Separation of two conductances in dentate granule cell EPSCs

The data clearly demonstrate the dual-component nature of the glutamatergic EPSCs in dentate granule cells. Similar to the results in hippocampal pyramidal cells (Hestrin *et al.* 1990), the fast, CNQX-sensitive and APV-insensitive component is mediated by a non-NMDA receptor conductance that displays a linear *I–V* relation. Most of the slow, CNQX-insensitive and APV-sensitive EPSC component is carried through an NMDA receptor conductance, which displays a region of negative slope conductance between −90 and −30 mV in the *I–V* relation. The increase in the relative contribution of this non-linear component with depolarization explains the deviation from linearity in the peak *I–V* relation of the natural EPSC. Granule cells whose peak *I–V* relation contains a region of negative slope conductance (Fig. 3)

probably have a larger fraction of synaptic NMDA receptor channels than cells with a more linear peak *I–V* curve (Fig. 9). Variations in the proportion of postsynaptic non-NMDA to NMDA receptor channels in single glutamatergic synapses have been recently demonstrated in cultured hippocampal neurones (Bekkers & Stevens, 1989).

The average contribution of the NMDA receptor conductance at −60 mV (in 1 mM Mg^{2+}) to the peak EPSC was quite substantial ($32 \pm 14\%$; n = 11). Indeed, binding studies have shown that NMDA receptors on adult rat dentate granule cells are abundant (Monaghan & Cotman, 1985). However, a previous study suggested that they are normally non-functional even in Mg^{2+}-free saline (Mody, Stanton & Heinemann, 1988). Since synaptic inhibition was not blocked in that study, it is possible that conjointly activated inhibitory postsynaptic potentials curtailed slow EPSP components (cf. Collingridge, Herron & Lester, 1988*a*, *b*). Indeed, when non-NMDA-mediated EPSP components were blocked with CNQX, which also suppresses excitation of feedforward inhibitory interneurones (Andreasen *et al.* 1989), a prominent NMDA-mediated EPSP component was uncovered in dentate granule cells in normal [Mg^{2+}] (Lambert & Jones, 1989). An NMDA-mediated EPSP component in EAA-operated synapses in normal Mg^{2+} has also been shown in other cortical regions (Thomson, 1986; Jones, 1987; Andreasen *et al.* 1988, 1989), in the thalamus (Salt, 1986), the spinal cord (Dale & Grillner, 1986; Konnerth, Keller & Lev-Tov, 1990*a*) and in cultures of CNS neurones (Forsythe & Westbrook, 1988).

Kinetics of non-NMDA EPSCs and their underlying molecular mechanism

The major component of the non-NMDA EPSCs decayed with a single time constant ranging from 3 to 9 ms. These values are significantly longer than the decay time below 1 ms found in cultured spinal cord neurones (Nelson, Pun & Westbrook, 1986), but are comparable to the decay found in whole-cell-clamped hippocampal pyramidal cells (7·1 ms; Hestrin *et al.* 1990), cerebellar Purkinje cells (3–8 ms; Konnerth, Llano & Armstrong, 1990*c*; Llano *et al.* 1990) and spinal cord motoneurones (2–5 ms; Konnerth *et al.* 1990*b*). The possibility that the slow decay is due to distortion of EPSCs by the cable properties of the neurones is rendered unlikely by the analysis of the passive cable properties of these cells (Hestrin *et al.* 1990; Llano *et al.* 1990). Instead, these results suggest that there is an intrinsic heterogeneity in EPSC decay, possibly due to a tissue-specific heterogeneity in glutamate receptor subunit composition (Hollmann, O'Shea-Greenfield, Rogers & Heinemann, 1989).

The molecular mechanisms controlling the time course of fast EPSCs can be investigated by comparing whole-cell synaptic currents with the underlying single-channel activity. Particularly useful proved to be the fast application of agonists to excised patches containing glutamate receptor channels (Franke, Hatt & Dudel, 1987; Dudel, Franke, Hatt, Ramsey & Usherwood, 1988; Tang, Dichter & Morad, 1989; Trussel & Fischbach, 1989). A large, rapidly inactivating glutamate receptor channel with a conductance of 36 pS and desensitization time constants of 3–8 ms was found in cultured hippocampal neurones (Tang *et al.* 1989) and could represent the 'subsynaptic' receptor channel mediating non-NMDA synaptic transmission (Trussel & Fischbach, 1989). The numerical similarity suggests, also, that the decay time constants of non-NMDA EPSCs (3–9 ms) in granule cells may be controlled

by receptor desensitization (time constant of 3–8 ms), although further direct experiments are needed to critically test this hypothesis.

Kinetic analysis of NMDA EPSCs and their underlying single-channel activity

The characteristic features of the NMDA EPSCs in dentate granule cells were the slow rise and decay times. The slow time course of NMDA-mediated synaptic responses in these and in other glutamatergic synapses was noted before in recordings obtained with intracellular microelectrodes (Andreasen *et al.* 1988; Blake *et al.* 1988; Collingridge *et al.* 1988*a*, *b*; Forsythe & Westbrook, 1988) and in the patch clamp whole-cell configuration (Hestrin *et al.* 1990; Konnerth *et al.* 1990*a*, *b*). Our results indicate that the decay of NMDA EPSCs is separable in two exponential components. The time constants of these two components were voltage dependent and were around 50 and 240 ms in normal saline at −70 mV. They increased to about 85 and 333 ms, respectively, upon removing Mg^{2+} from the perfusion solution. Washing the preparations with nominally Mg^{2+}-free solutions reduced, but did not entirely abolish, the voltage sensitivity of NMDA EPSC decay. Thus a substantial part of this voltage sensitivity is conferred by a blocking action of extracellular Mg^{2+} (Mg_o^{2+}) (Konnerth *et al.* 1990*b*). Whether the remaining voltage sensitivity is due to residual Mg_o^{2+} or to an intrinsic voltage sensor of the NMDA receptor channel protein has yet to be determined.

The ionic channels underlying NMDA EPSCs were investigated in outside-out patch clamp experiments from hippocampal granule cells. Such measurements revealed the existence of single NMDA receptor channels with a main conductance level of 52 pS, which is in good agreement with previously reported values for NMDA receptor channels in cultured neurones (Cull-Candy & Usowicz, 1987; Jahr & Stevens, 1987; Ascher, Bregestovski & Nowak, 1988). This observation is remarkable, since for other types of ligand-gated channels there is less similarity in the single-channel conductances in cultured neurones compared to well differentiated neurones in slices. For example, GABA-activated channels in cultured neurones display four distinct conductance levels (Bormann, Hamill & Sakmann, 1987), while granule cells in hippocampal slices display two main conductance states (Edwards, Konnerth & Sakmann, 1990).

The duration of NMDA EPSCs in hippocampal granule cells (several hundreds of milliseconds, see Fig. 7) greatly exceeds the mean open times (4–6 ms), and the mean burst lengths (10–17 ms) of NMDA receptor channels (Cull-Candy & Usowicz, 1987, 1989*b*; Ascher *et al.* 1988; Ascher & Nowak, 1988; Howe, Colquhoun & Cull-Candy, 1988). This indicates that in the case of NMDA EPSCs, the mean burst length of channel openings is not the 'elementary event' that determines the decay of these currents. Instead, our results support the notion that clusters of bursts of NMDA receptor channels which could last several hundreds of milliseconds represent more suitable candidates for the underlying elementary single-channel event (see also Jahr & Stevens, 1987; Howe *et al.* 1988). This is strongly supported by recent experiments in cultured hippocampal neurones (Lester, Clements, Westbrook & Jahr, 1990), which show that pulse-like applications of glutamate to outside-out patches induce long-lasting clusters of NMDA receptor channel openings.

Implications for neural function

Our data corroborate the notion that the NMDA EPSC component contributes a small but significant component to the peak EPSC at resting membrane potential, and thus may play a role in normal impulse transmission across the glutamate synapse. Moreover, already at resting potential this component accounts for most of the charge transferred during an EPSC (Fig. 9*C*). Furthermore, by virtue of its apparent voltage sensitivities, this component underlies the huge increase in synaptic charge transfer, and hence, Ca^{2+} entry, upon depolarization. This behaviour may explain the specific roles of NMDA receptors in several forms of neural plasticity, namely long-term potentiation of excitatory synaptic transmission, kindling, epileptic seizures and neuronal degeneration consequent to ischaemia, hypoxia and trauma (for review see Collingridge & Bliss, 1987; Mayer & Westbrook, 1987; Choi, 1988; Monaghan, Bridges & Cotman, 1989).

We thank F. Friedlein for excellent technical assistance. This work was supported by the Deutsche Forschungsgemeinschaft (SFB 236), by the Bundesministerium für Forschung und Technologie, by a Twinning Grant from the European Science Foundation and by a Grant from the German–Israeli Foundation (GIF) for Scientific Research and Development.

REFERENCES

ANDERSEN, P. O. (1987). Properties of hippocampal synapses of importance for integration and memory. In *Synaptic Function*, ed. EDELMAN, G. M., GALL, W. E. & COWAN, W. M., pp. 403–429. John Wiley & Sons, New York.

ANDREASEN, M., LAMBERT, J. D. C. & JENSEN, M. S. (1988). Direct demonstration of an *N*-methyl-D-aspartate mediated component of excitatory synaptic transmission in area CA1 of the rat hippocampus. *Neuroscience Letters* **93**, 61–66.

ANDREASEN, M., LAMBERT, J. D. C. & JENSEN, M. S. (1989). Effects of new non-*N*-methyl-D-aspartate antagonists on synaptic transmission in the *in vitro* rat hippocampus. *Journal of Physiology* **414**, 317–336.

ASCHER, P., BREGESTOVSKI, P. & NOWAK, L. (1988). *N*-Methyl-D-aspartate-activated channels of mouse central neurones in magnesium-free solutions. *Journal of Physiology* **399**, 207–226.

ASCHER, P. & NOWAK, L. (1988). The role of divalent cations in the *N*-methyl-D-aspartate responses of mouse central neurones in culture. *Journal of Physiology* **399**, 247–266.

BEKKERS, J. M. & STEVENS, C. F. (1989). NMDA and non-NMDA receptors are co-localized at individual excitatory synapses in cultured rat hippocampus. *Nature* **341**, 230–233.

BLAKE, J. F., BROWN, M. W. & COLLINGRIDGE, G. L. (1988). CNQX blocks acidic amino acid induced depolarizations and synaptic components mediated by non-NMDA receptors in rat hippocampal slices. *Neuroscience Letters* **89**, 182–186.

BORMANN, J., HAMILL, O. P. & SAKMANN, B. (1987). Mechanism of anion permeation through channels gated by glycine and γ-aminobutyric acid in mouse cultured spinal neurones. *Journal of Physiology* **385**, 243–286.

CHOI, D. W. (1988). Glutamate neurotoxicity and diseases of the nervous system. *Neuron* **1**, 623–634.

COLLINGRIDGE, G. L. & BLISS, T. V. P. (1987). NMDA-receptors – their role in long-term potentiation. *Trends in Neurosciences* **10**, 288–293.

COLLINGRIDGE, G. L., HERRON, C. E. & LESTER, R. A. J. (1988*a*). Synaptic activation of *N*-methyl-D-aspartate receptors in the Schaffer collateral–commissural pathway of rat hippocampus. *Journal of Physiology* **399**, 283–300.

COLLINGRIDGE, G. L., HERRON, C. E. & LESTER, R. A. J. (1988*b*). Frequency-dependent *N*-methyl-D-aspartate receptor-mediated synaptic transmission in rat hippocampus. *Journal of Physiology* **399**, 301–312.

CRUNELLI, V., FORDA, S. & KELLY, J. S. (1984). The reversal potential of excitatory amino acid action on granule cells of the rat dentate gyrus. *Journal of Physiology* **351**, 327–342.

CULL-CANDY, S. G. & USOWICZ, M. M. (1987). Multiple-conductance channels activated by excitatory amino acids in cerebellar neurones. *Nature* **325**, 525–528.

CULL-CANDY, S. G. & USOWICZ, M. M. (1989*a*). Whole-cell current noise produced by excitatory and inhibitory amino acids in large cerebellar neurones of the rat. *Journal of Physiology* **415**, 533–553.

CULL-CANDY, S. G. & USOWICZ, M. M. (1989*b*). On the multiple-conductance single channels activated by excitatory amino acids in large cerebellar neurones of the rat. *Journal of Physiology* **415**, 555–582.

DALE, N. & GRILLNER, S. (1986). Dual-component synaptic potentials in the lamprey mediated by excitatory amino acid receptors. *Journal of Neuroscience* **6**, 2653–2661.

DUDEL, J., FRANKE, CH., HATT, H., RAMSEY, R. & USHERWOOD, P. N. R. (1988). Rapid activation and desensitization by glutamate of excitatory, cation-selective channels in locust muscle. *Neuroscience Letters* **88**, 33–38.

EDWARDS, F. A., KONNERTH, A. & SAKMANN, B. (1990). Quantal synaptic transmission in the central nervous system: A patch clamp study of IPSCs in rat hippocampal slices. *Journal of Physiology* **430**, 213–249.

EDWARDS, F. A., KONNERTH, A., SAKMANN, B. & TAKAHASHI, T. (1989). A thin slice preparation for patch clamp recordings from neurones of the mammalian central nervous system. *Pflügers Archiv* **414**, 600–612.

FORSYTHE, I. D. & WESTBROOK, G. L. (1988). Slow excitatory postsynaptic currents mediated by *N*-methyl-D-aspartate receptors on cultured mouse central neurones. *Journal of Physiology* **396**, 515–533.

FRANKE, CH., HATT, H. & DUDEL, J. (1987). Liquid filament switch for ultra-fast exchanges of solutions at excised patches of synaptic membrane of crayfish muscle. *Neuroscience Letters* **77**, 199–204.

HABLITZ, J. J. & LANGMOEN, I. A. (1982). Excitation of hippocampal pyramidal cells by glutamate in the guinea-pig and rat. *Journal of Physiology* **325**, 317–331.

HAMILL, O. P., MARTY, A., NEHER, E., SAKMANN, B. & SIGWORTH, F. J. (1981). Improved patch-clamp techniques for high-resolution current recording from cells and cell-free membrane patches. *Pflügers Archiv* **391**, 85–100.

HESTRIN, S., NICOLL, R. A., PERKEL, D. J. & SAH, P. (1990). Analysis of excitatory synaptic action in pyramidal cells using whole-cell recording from rat hippocampal slices. *Journal of Physiology* **422**, 203–225.

HOLLMANN, M., O'SHEA-GREENFIELD, A., ROGERS, S. W. & HEINEMANN, S. (1989). Cloning by functional expression of a member of the glutamate receptor family. *Nature* **342**, 643–648.

HONORÉ, T., DAVIES, S. N., DREJER, J., FLETCHER, E. J, JACOBSEN, P., LODGE, D. & NIELSEN, F. E. (1988). Quinoxalinediones: potent competitive non-NMDA glutamate receptor antagonists. *Science* **241**, 701–703.

HOWE, J. R., COLQUHOUN, D. & CULL-CANDY, S. G. (1988). On the kinetics of large-conductance glutamate receptor ion channels in rat cerebellar granule neurones. *Proceedings of the Royal Society* B **233**, 407–422.

JAHR, C. E. & STEVENS, C. F. (1987). Glutamate activates multiple single channel conductances in hippocampal neurones. *Nature* **325**, 522–525.

JONES, R. S. G. (1987). Complex synaptic responses of entorhinal cortical cells in the rat to subicular stimulation *in vitro*: demonstration of an NMDA receptor-mediated component. *Neuroscience Letters* **81**, 209–214.

KELLER, B. U., YAARI, Y. & KONNERTH, A. (1990). Kinetic analysis of excitatory postsynaptic currents in hippocampal granule cells. *Pflügers Archiv* **415**, suppl. 1, 68.

KONNERTH, A., KELLER, B. U., BALLANYI, K. & YAARI, Y. (1990*a*). Voltage sensitivity of NMDA-receptor mediated postsynaptic currents. *Experimental Brain Research* **81**, 209–212.

KONNERTH, A., KELLER, B. U. & LEV-TOV, A. (1990*b*). Patch-clamp analysis of excitatory synapses in mammalian spinal cord slices. *Pflügers Archiv* **417**, 285–290.

KONNERTH, A., LLANO, I. & ARMSTRONG, C. M. (1990*c*). Synaptic currents in cerebellar Purkinje cells. *Proceedings of the National Academy of Sciences of the USA* **87**, 2662–2665.

LAMBERT, J. D. C. & JONES, R. S. G. (1989). Activation of *N*-methyl-D-aspartate receptors contributes to the EPSP at perforant path synapses in the rat dentata gyrus in vivo. *Neuroscience Letters* **97**, 323–328.

LESTER, R. A. J., CLEMENTS, J. D., WESTBROOK, G. L. & JAHR, C. E. (1990). Channel kinetics determine the time course of NMDA receptor-mediated synaptic currents. *Nature* **346**, 565–567.

LLANO, I., MARTY, A., ARMSTRONG, C. M. & KONNERTH, A. (1991). Synaptic- and agonist-induced excitatory currents of Purkinje cells in rat cerebellar slices. *Journal of Physiology* **434**, 183–213.

LØMO, T. (1971). Patterns of activation in a monosynaptic cortical pathway: The perforant path input to the dentate area of the hippocampal formation. *Experimental Brain Research* **12**, 18–45.

MACDERMOTT, A. B., MAYER, M. L., WESTBROOK, G. L., SMITH, S. J. & BARKER, J. L. (1986). NMDA-receptor activation increases cytoplasmic calcium concentration in cultured spinal cord neurones. *Nature* **321**, 519–522.

MARTELL, A. E. & SMITH, R. M. (1974). *Critical Stability Constants*, vol. 2, *Amines*, p. 283. Plenum Press, New York.

MAYER, M. L. & WESTBROOK, G. L. (1987). The physiology of excitatory amino acids in the vertebrate central nervous system. *Progress in Neurobiology* **28**, 197–276.

MAYER, M., WESTBROOK, G. L. & GUTHRIE, P. B. (1984). Voltage-dependent block by Mg^{2+} of NMDA responses in spinal cord neurones. *Nature* **309**, 261–263.

MODY, I., SALTER, M. W. & MACDONALD, J. F. (1988). Requirement of NMDA receptor/channels for intracellular high-energy phosphates and the extent of intraneuronal calcium buffering in cultured mouse hippocampal neurones. *Neuroscience Letters* **93**, 73–78.

MODY, I., STANTON, P. K. & HEINEMANN, U. (1988). Activation of *N*-methyl-D-aspartate receptors parallels changes in cellular and synaptic properties of dentate gyrus granule cells after kindling. *Journal of Neurophysiology* **59**, 1033–1054.

MONAGHAN, D. T., BRIDGES, R. J. & COTMAN, C. W. (1989). The excitatory amino acid receptors: Their classes, pharmacology, and distinct properties in the function of the central nervous system. *Annual Review of Pharmacology and Toxicology* **29**, 356–402.

MONAGHAN, D. T. & COTMAN, C. W. (1985). Distribution of NMDA-sensitive L-^{3}H-glutamate binding sites in rat brain as determined by quantitative autoradiography. *Journal of Neuroscience* **5**, 2909–2919.

NELSON, P. G., PUN, R. Y. K. & WESTBROOK, G. L. (1986). Synaptic excitation in cultures of mouse spinal cord neurones: receptor pharmacology and behaviour of synaptic currents. *Journal of Physiology* **372**, 169–190.

NOWAK, L., BREGESTOVSKI, P., ASCHER, P., HERBET, A. & PROCHIANTZ, A. (1984). Magnesium gates glutamate-activated channels in mouse central neurones. *Nature* **307**, 462–465.

SALT, T. E. (1986). Mediation of thalamic sensory input by both NMDA and non-NMDA receptors. *Nature* **322**, 263–265.

TANG, C.-M., DICHTER, M. & MORAD, M. (1989). Quisqualate activates a rapidly inactivating high conductance ionic channel in hippocampal neurones. *Science* **243**, 1474–1477.

THOMSON, A. M. (1986). A magnesium-sensitive post-synaptic potential in rat cerebral cortex resembles neuronal responses to *N*-methyl-D-aspartate. *Journal of Physiology* **370**, 531–549.

TRUSSEL, L. O. & FISCHBACH, G. D. (1989). Glutamate receptor desensitisation and its role in synaptic transmission. *Neuron* **3**, 209–218.

WATKINS, J. C. & EVANS, R. H. (1981). Excitatory amino acid transmitters. *Annual Review of Pharmacology and Toxicology* **21**, 165–204.

WATKINS, J. C. & OLVERMAN, H. J. (1987). Agonists and antagonists for excitatory amino acid receptors. *Trends in Neurosciences* **10**, 265–272.